

PAPER • OPEN ACCESS

Propagation of the phase-modulated femtosecond pulses through the optically-dense quasi-resonant medium

To cite this article: A A Preobrazhenskaia *et al* 2018 *J. Phys.: Conf. Ser.* **1038** 012071

View the [article online](#) for updates and enhancements.

Related content

- [Fraunhofer type diffraction of phase-modulated broad-band femtosecond pulses](#)
A M Dakova, L M Kovachev, K L Kovachev *et al.*
- [Coherent propagation of a short polarised radiation pulse in a one-dimensional resonance Bragg grating](#)
Andrei I Maimistov and V V Polikarpov
- [Propagation of femtosecond pulses in a hollow-core revolver fibre](#)
Yu P Yatsenko, A A Krylov, A D Pryamikov *et al.*

Propagation of the phase-modulated femtosecond pulses through the optically-dense quasi-resonant medium

A A Preobrazhenskaia¹, A A Pastor¹, P Yu Serdobintsev¹, I A Chekhonin¹, V S Egorov¹

¹St. Petersburg State University, St. Petersburg, Russia

E-mail: nakozina_alena@inbox.ru

Abstract. It is known that ultrashort pulse coherent propagation through the resonant absorbing medium leads to the pulse splitting and pulse train generation. First of these pulses is the input pulse and the following pulses are resonant medium response. It is also known that such a propagation mode leads to the «spectrum condensation» effect, at which broad-band input femtosecond laser emission, as it leaves optically-dense medium, centralized in the vicinity of the resonance absorption lines. It's interesting to clear up the dependence of a condensation effect on an input femtosecond pulse phase modulation value (chirp).

1. Introduction

Coherent propagation of an ultrashort pulse through the optically-dense rubidium vapors under the quasi-resonant conditions is studied. Hence the early published articles [1,2] concerned the data of these processes without chirping of the incident laser pulse it is interesting to elucidate the chirping influence on the transformation of an outgoing pulse. The brief results of the experiments combined with the computer simulation are presented below.

In our investigation we used the femtosecond laser «Pulsar-10» with the following parameters: pulse duration – 50 fs, pulse energy – up to 10 mJ, carrier wavelength – 790 nm, pulse spectrum half-width – about 20 nm, light intensity – 0.1 TW/cm², beam diameter – 5 mm. To generate phase modulation the compressor, consisted of 2 of diffraction gratings, with changeable distances between them, was used.

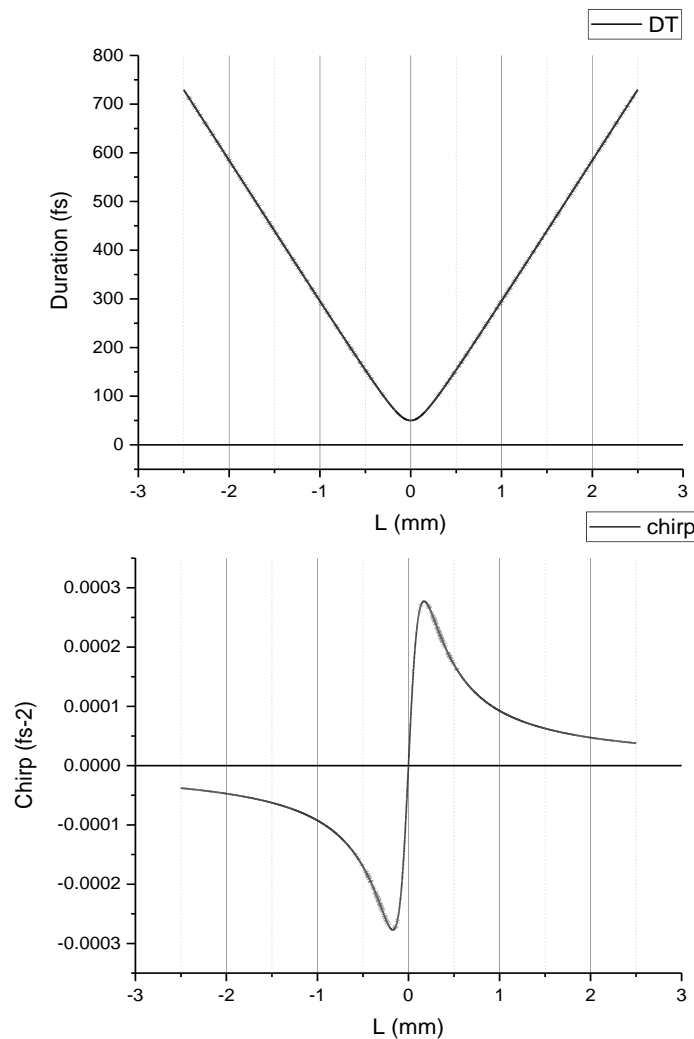
As a resonant medium the cell (length – 10 cm, diameter – 3 cm) with Rb vapor and buffer gas Ar was taken. To get required Rb vapor pressure we heated the cell to 200-300 °C. Concentration of vapor is about 10¹⁶ cm⁻³.

The femtosecond laser «Pulsar-10» was consisted of the oscillator, stretcher, amplifier and compressor, comprised 2 diffraction gratings. Output pulse chirping was attained due to the changing of a distance between these 2 diffraction gratings. Group Delay Dispersion (GDD) was given by following dependence:

$GDD(L) = 5250 * L(\text{mm}) [\text{fs}^2]$, where L – distance between the gratings, measured with relation to the position, when chirp is 0.

Dependence of the pulse duration and chirp on the compressor detuning is shown in figures 1 and 2 correspondingly.





Figures 1 and 2. Dependence of the pulse duration and chirp on the compressor detuning.

Figure 1 shows the pulse half-width changing, depending on the detuning, giving by the following expression:

$$\Delta t^2 = (\Delta t_0^4 + 16(\ln 2)^2 \cdot \text{GDD}^2) / \Delta t_0^2$$

where Δt_0 – pulse half-width in case of compressor zero detuning.

Figure 2 shows the dependence of the chirp on the detuning, giving by the following dependence:

$$\text{Chirp} = 8 (\ln 2)^2 \cdot \text{GDD} / (\Delta t_0^4 + 16(\ln 2)^2 \cdot \text{GDD}^2)$$

The results of our experiment show us that a response time of a resonant medium to an input pulse is highly sensitive to a phase modulation sign (chirp). It leads whether to an input signal and a response medium signal constructive interference or, as the result of the change of a chirp sign, to a destructive interference. Examples of the «condensation» and «anti-condensation» of the femtosecond pulse, passed through the Rb vapor cell, were registered on the Rb resonance line (wavelength is 780 nm) in the setting of different chirp signs and are shown in figures 3 and 4.

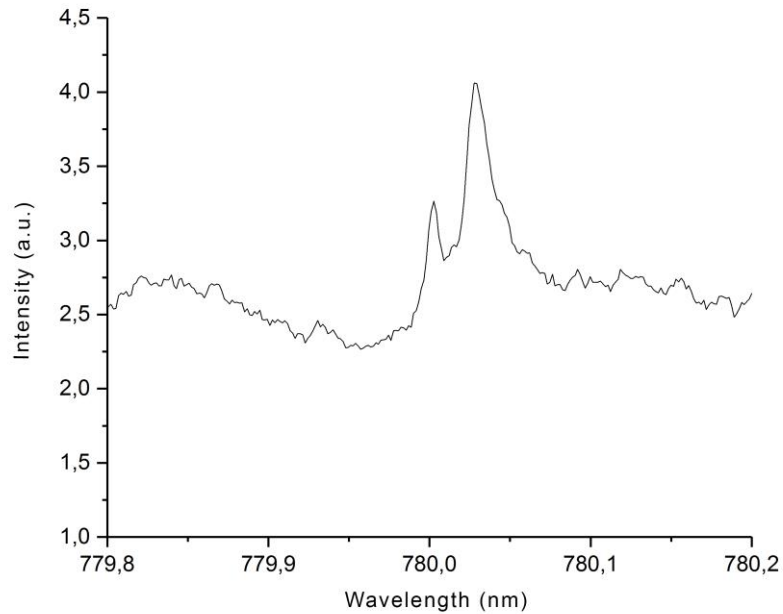


Figure 3. «Spectrum condensation» effect in the vicinity of the Rb resonance line (wavelength is 780 nm). GDD= -2610 fs².

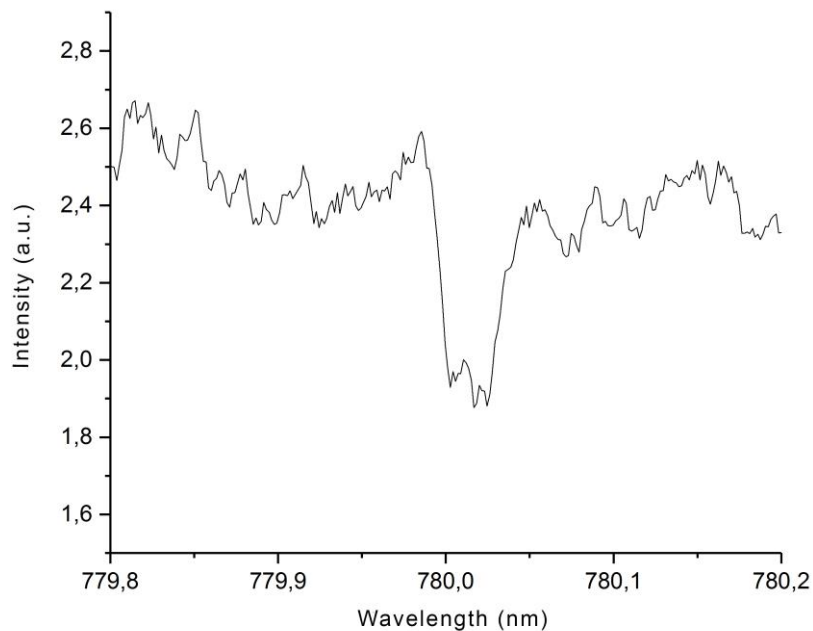


Figure 4. «Spectrum anti-condensation» effect in the vicinity of the Rb resonance line (wavelength is 780 nm). GDD= 2610 fs².

It is apparent that under negative chirp value the «spectrum anti-condensation» (spectrum notches in the vicinity of the absorption line, caused by destructive train pulses interference) is observed.

Spectra of laser emission, got through the rubidium cell in «spectrum condensation» regime, was registered with the high resolution spectrograph DFS-8 with a diffraction grating with following parameters: 1200 grooves per mm, dispersion – 0.4 nm/mm. Laser emission spectrum half-width was

20 nm. We used CCD camera with the 7 mm matrix (1000 pixels) for the registration, so the spectral region with a width of 2 nm was registered and it wasn't possible to register the whole spectrum. Panoramic spectrum was registered with the Ocean Optics spectrometer (instrumental width – 0.5 nm). This spectrum is shown in figure 5.

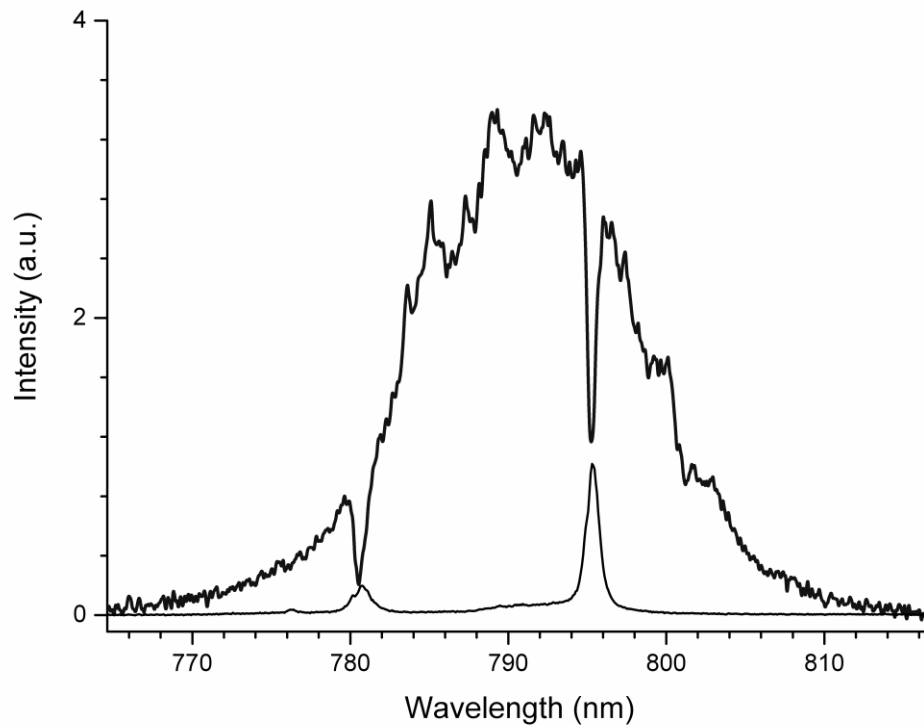


Figure 5. Panoramic spectrum, registered with the Ocean Optics spectrometer.

Upper spectrogram shows the laser spectrum, obtained through the rubidium cell in incoherent propagation conditions. To get these conditions laser beam passed through the teflon diffuser before the cell. You can see 2 rubidium resonance doublet absorption lines. Lower spectrogram shows the laser spectrum, got through the rubidium cell in coherent propagation conditions (without the diffuser). You can see the spectrum condensation effect in the vicinity of the rubidium lines. Condensation effect, as it seen from the panoramic spectrum, become apparent on the both lines (D_1 and D_2) of the rubidium resonance doublet.

Rubidium vapor, consisted of the natural isotopic mixture with the atomic weight 85 and 87, was used. But isotopic splitting of the D_1 and D_2 rubidium lines is much less than the observed line width of the spectra condensation (and anti-condensation).

«Spectrum condensation» effect can be observed with 2 types of emission spectrum on a frequency of the resonant atomic transition. In the case of low density of the rubidium atoms N_0 the narrow superradiance line on a frequency of an atomic resonance ω_{12} is observed. In case of atomic concentration increasing, the intensity of resonance emission increases.

But from some threshold value N_0 , the emission spectrum of the atomic ensemble splits into 2 satellites [2]. Their frequency slitting value is defined by the value of the polariton mode frequency splitting value in the resonant medium and increases as N_0 increases.

2. Results of the computer simulation.

We give here some of the model calculations of the resonant absorbing medium polarization response to the femtosecond excitation pulse by taking into account resonance transition frequency detuning in response to the different sign of the input pulse phase modulation.

Model used for computer simulation and obtained results can be described in the following way.

Bloch equations – equations, described precession of the vector ρ around vector Ω .

$$\frac{d\rho}{dt} = [\Omega \times \rho]$$

$$\Omega = [-\Omega_{R_1}, -\Omega_{R_2}, \Delta] - \text{pump field control vector.}$$

$$\rho = [u, v, w] - \text{Bloch vector.}$$

Without relaxation ($T_1 = T_2 = \infty$) Bloch vector's squared length is $|\rho|^2 = u^2 + v^2 + w^2 = 1$.

Bloch equations for the projections ρ by taking into account phenomenological decay time T_1 and T_2 :

$$du/dt = -\Delta v - u/T_2 - \Omega_{R_2} w$$

$$dv/dt = \Delta u - v/T_2 + \Omega_{R_1} w$$

$$dw/dt = -(w - w_{eq})/T_1 - \Omega_{R_2} u - \Omega_{R_1} v$$

Slow envelope curve of the medium polarization $P = d_{12} N_0 (u + iv)$.

d_{12} – matrix element of the dipole moment operator.

$w = N/N_0$ – normalized population difference.

w_{eq} – equilibrium normalized population difference.

In this case $w_{eq} = -1$.

$\Omega_R = \Omega_{R_1} + i\Omega_{R_2}$ – complex Rabi frequency.

$$\Omega_R = d_{12} E/\hbar, E = E_1 + iE_2$$

$\Delta(t) = \omega_{12} - \omega(t)$, $\Delta(t) = \Delta_0 + (d\Delta(t)/dt)t$ – current laser frequency detuning.

$d\Delta(t)/dt$ – chirp.

Δ_0 – laser pulse frequency detuning without chirp.

All the calculations were made in arbitrary units. But in fact only magnitude relation of $|\Omega_R|$, pulse duration 2σ , Δ_0 , T_1 , T_2 and chirp $d\Delta(t)/dt$ are important.

Knowing pulse duration and detuning values, we can estimate effects in real conditions.

$|\Omega_R| = 3$, pulse duration $2\sigma = 3$, frequency laser detuning from exact position of an atomic resonance ω_{12} without chirp $\Delta_0 = 20$, $T_1 = T_2 = 10$.

In figures 6-11 the field amplitude $|E(t)|$ during the pulse is shown. Medium polarization $|u(t) + iv(t)|$ is given in arbitrary units.

In this thin medium layer model the polarization superradiance effect is absent, that's why it decays only by virtue of relaxation (T_1 and T_2 are finite).

In accordance with the above-described model some analytical data for different sign and values of the chirp is presented below.

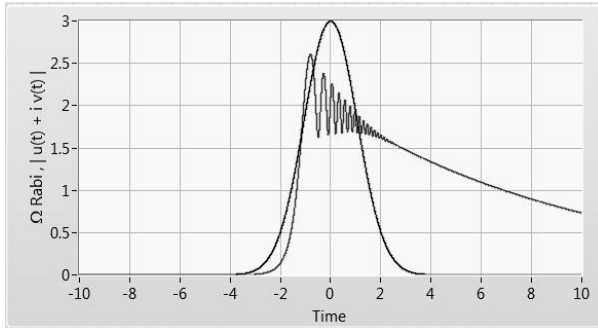


Figure 6. Polarization time dependence in a thin layer on input pulse. The chirp is +15.

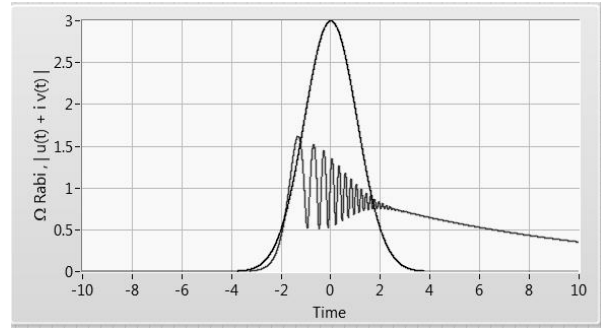


Figure 7. Polarization time dependence in a thin layer on input pulse. The chirp is +10.

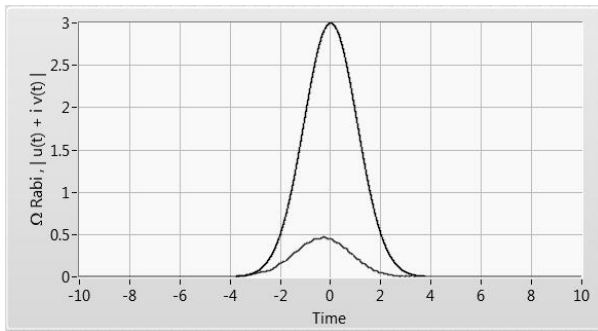


Figure 8. Polarization time dependence in a thin layer on input pulse. The chirp is +5.

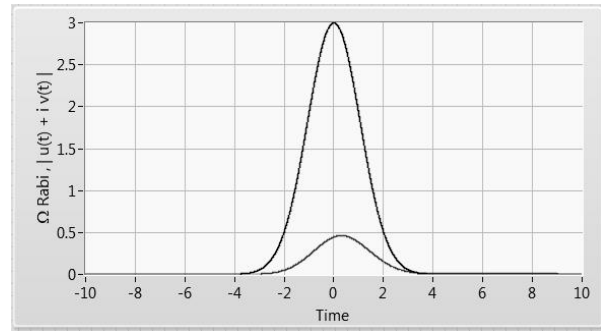


Figure 9. Polarization time dependence in a thin layer on input pulse. The chirp is -5.

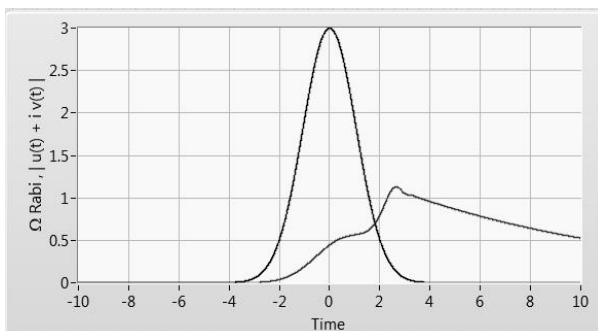


Figure 10. Polarization time dependence in a thin layer on input pulse. The chirp is -10.

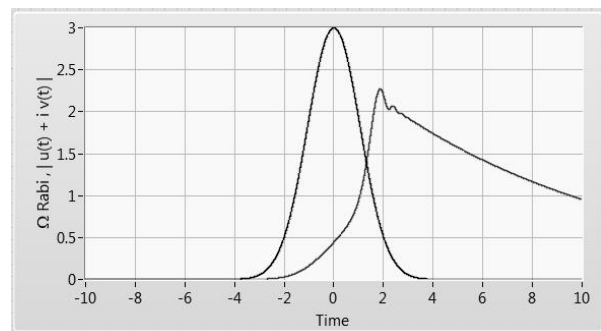


Figure 11. Polarization time dependence in a thin layer on input pulse. The chirp is -15.

In the case of the non-adiabatic excitation of the medium polarization, the superradiant pulse of the rubidium atom ensemble occurs. It's important to say that this superradiant radiation type can occur without achievement of the population inversion w of the resonant medium.

The result of the excitation pulse and superradiant pulse interference is defined by the phase difference of the field oscillation of the excitation pulse and superradiant pulse on the resonance frequency ω_{12} : $\Delta\varphi_1 = \varphi_1 - \text{atan}[v(t_1)/u(t_1)]$ and $\Delta\varphi_2 = \varphi_2 - \text{atan}[v(t_2)/u(t_2)]$, where t_1 and t_2 - time moments, when medium induced polarization amplitude $|u(t) + iv(t)|$ achieves its' maximum for the negative and positive chirp sign, accordingly; φ_1 and φ_2 - excitation pulse oscillation phases on the frequency ω_{12} in the time moment t_1 and t_2 . Constructive interference condition is $\Delta\varphi_1 = 0$, destructive interference condition is $\Delta\varphi_2 = \pm \pi$.

3. Conclusion

As can be seen from the computer modeling in figures 6-11, the chirp sign change leads to the radical change of polarization response. In the case of a positive chirp the polarization response appears on the pulse leading edge, and in the case of a negative chirp the substantial delay of the polarization response is observed. We are of the opinion that this delay is the major cause of the transfer from constructive to destructive interference of the pulse train, passing through the optically-dense medium.

Acknowledgements

V.S.E. and I.A.C. thanks Russian Science Foundation (project 17-19-01097) for the partial support of numerical simulations.

Part of the experiments were performed out in the Research Resource Center “Physical methods of surface investigation” of Saint Petersburg State University.

References

- [1] Rothenberg J E, Grischkovsky D, Balant A C 1984 Phys.Rev.Lett. **53** (6) 552-555;
- [2] Bagaev S N, Egorov V S, Pastor A A, Preobrazhenskii D Yu, Preobrazhenskaya A A, Serdobintsev P Yu, Chekhonin I A, Chekhonin M A 2016 Opt. Spectr. **121** (3) 391-394